Large-Scale Ocean–Atmosphere Interactions in a Simplified Coupled Model of the Midlatitude Wintertime Circulation

ARTHUR J. MILLER

Climate Research Division, Scripps Institution of Oceanography and California Space Institute, University of California, San Diego, La Jolla, California

(Manuscript received 31 August 1990, in final form 31 May 1991)

ABSTRACT

Midlatitude ocean–atmosphere interactions are studied in simulations from a simplified coupled model that includes synoptic-scale atmospheric variability, ocean current advection of sea surface temperature (SST), and air–sea heat exchange. Although theoretical dynamical ("identical twin") predictions using this model have shown that the SST anomalies in this model indeed influence the atmosphere, we find here that standard cross-correlation and empirical orthogonal function analyses of monthly mean model output yield the standard result, familiar from observational studies, that the atmosphere forces the ocean with little or no feedback. Therefore, these analyses are inconclusive and leave open the question of whether anomalous SST is influencing the atmosphere. In contrast, we find that compositing strong warm events of model SST is a useful indicator of ocean forcing the atmosphere. We present additional evidence for oceanic influence on the atmosphere, namely, that ocean current advection appears to enhance the persistence of model SST anomalies through a feedback effect that is absent when only heat flux is allowed to influence SST anomaly evolution. Models with more complete physics must ultimately be used to conclusively demonstrate these results.

1. Introduction

The importance of midlatitude sea surface temperature (SST) anomalies in the seasonal variability and predictability of the atmosphere has been explored and debated for decades (e.g., Namias 1972a, 1976; Davis 1976, 1978; Chervin et al. 1980; Palmer and Sun 1985; Pitcher et al. 1988; Lau and Nath 1990; and Frankignoul 1985 reviews the subject). Observational analyses of monthly and/or seasonal mean data have revealed strong correlation between SST and atmospheric variables when the atmosphere leads, and a somewhat weaker contemporaneous correlation. However, the observations show that when the ocean leads the atmosphere by one month and longer, there is a very weak correlation between the two systems. These results suggest that the primary connection between midlatitude ocean and atmosphere is "atmosphere forcing ocean," although the slow oceanic influence may simply be very difficult to pinpoint in observations. Indeed, as Namias (1978) described the situation, "It is much easier to show that the atmosphere influences SST than vice versa."

Various numerical modeling studies have therefore attempted to reveal the "ocean forcing atmosphere" side of the coin. By specifying fixed midlatitude SST anomalies as boundary conditions in sophisticated climate models, the perturbation of the mean flow field of the atmospheric model can be computed and tested for significance. Although some of the earlier numerical studies showed a weaker contemporaneous atmospheric response than observations would suggest, recent numerical model results (e.g., Palmer and Sun 1985; Pitcher et al. 1988; and the study by Lau and Nath 1990, which used observed time-varying SST anomalies) suggest that the atmospheric perturbation is significant and comparable in amplitude with observed anomalies. However, the response of the atmosphere to midlatitude SST anomalies is not very large compared to the intrinsic variability of the atmosphere alone, which is why statistical significance is difficult to prove.

Although the numerical model experiments show that midlatitude SST anomalies can influence *contemporaneous* atmospheric flows, the usefulness of these SST anomalies in forecasts (ocean leading atmosphere) is less certain. The need for improving extended-range forecasting of atmospheric climate variations makes it imperative to study the coupled system to determine if some important facets of oceanic influence have been slighted.

Recently, Miller and Roads (1990) found that midlatitude SST anomalies significantly improved theoretical predictions[1] of atmospheric flow in a coupled

Corresponding author address: Arthur J. Miller, Scripps Institution of Oceanography, Climate Research Division, A-024, University of California, San Diego, La Jolla, CA 92093.

[1] When referring to theoretical dynamical predictions, we mean dynamical models predicting their own output with small error in the initial conditions ("identical twin" experiments).

model. When the evolving SST field was specified from model "observed" flows, the predictions of atmospheric time-averaged flow, for averages of one month and longer, were significantly enhanced over predictions based on the atmospheric model with climatological SST. Coupled simulations like these will ultimately help to verify the provocatively few observed indications of ocean forcing atmosphere (e.g., Namias 1976; Davis 1978). More important, coupled models will clarify the mechanisms involved, for, unlike the real climate system, we can alter the model systems to include and exclude key processes in the complexity of air–sea interactions.

For example, Palmer and Sun (1985) have suggested a mechanism of ocean–atmosphere interaction that may result in enhanced persistence of atmospheric anomalies in a coupled system. Their mechanism (which was adumbrated by Namias 1963) relies on the anomalous Ekman advection of warm water from the south by an anomalous atmospheric high, associated with a warm SST anomaly. The anomalous advection then reinforces the warm SST anomaly, which in turn reinforces the atmospheric anomaly. Does enhanced persistence occur in a coupled model, with synoptic-scale atmospheric variability, when it includes heat flux and ocean current advection, compared to a system that includes only heat flux in air–sea interaction?

As another example, Ratcliffe and Murray (1970) demonstrated oceanic influence by using composites of strong monthly mean SST anomalies of the Atlantic, off the coast of Newfoundland. They showed that, for *certain* fall/winter months, atmospheric circulation anomalies over the North Atlantic and Europe in the subsequent month are significantly correlated with the SST anomalies. Palmer and Sun (1985), however, computed similar composites of these SST observations that included *all* fall/winter months and found no significant composited atmospheric response in the subsequent month. If one applies the technique of compositing to the output from a coupled model, are the results of Ratcliffe and Murray substantiated?

Last, the negative results associated with cross-correlation analysis have been countered by the arguments of Wallace and Jiang (1987) who emphasize that, while the lagged cross correlation indicates an atmosphere forcing ocean, the contemporaneous cross correlation between SST and atmospheric fields may be indicative of an ocean forcing atmosphere because the atmospheric response is nearly instantaneous for monthly mean variables. In a coupled system in which the ocean significantly forces the atmosphere, do the standard negative results of cross-correlation analysis prevail?

As a first step in the direction of analyzing coupled models for large-scale, midlatitude, ocean–atmosphere interaction, we examine the output from two coupled models developed by Miller and Roads (1990) and described in section 2. One system includes only heat flux in SST evolution, while the second includes both heat flux and ocean current advection in SST variability. In section 3, we employ standard correlation and empirical orthogonal function (EOF) analyses to investigate and compare the large-scale ocean–atmosphere interactions that occur in the two coupled systems, and address the aforementioned questions. The results are summarized in section 4.

2. Coupled model description

The model output is taken from two of the simplified climate systems modeled by Miller and Roads (1990). The atmosphere is a perpetual January, Northern Hemispheric, quasigeostrophic, two-layer model with orography and steady empirically derived forcing as well as time-dependent forcing from surface heat flux. The heat flux is taken to be a linear function of the difference of SST and atmospheric temperature, T_a, proportional to the baroclinic streamfunction (500-mb temperature). The SST is calculated from a heat equation, namely,

$$\frac{\partial T}{\partial t} + \mathbf{u}\cdot\nabla T = K(T_a - T) + \kappa\nabla^2 T + F \quad (2.1)$$

for a mixed layer of constant 50-m depth, with K^{-1} = 58 days and κ = 500 m^2 s^{-1}. The surface current, $\mathbf{u}$, has two parts: the Ekman velocity, directly computed from and perpendicular to the atmospheric model wind stress, and geostrophic velocity, predicted by an underlying, quasigeostrophic, two-layer, flat-bottom North Pacific Ocean model, forced directly by the fluctuating wind stress curl. The steady forcing, F, is empirically computed and serves to maintain a realistic SST climatology. Heat flux and ocean current advection can affect SST in the North Pacific, while the Atlantic and Indian oceans are affected only by heat flux. Equatorial influences are *excluded* from these model systems. (See Miller and Roads 1990 for complete details of the models.)

For this study, we consider two coupled atmosphere–ocean climate systems within which:

(Case 1) heat flux alone drives the SST anomalies, and

(Case 2) both heat flux and ocean current advection influence Pacific SST anomalies.

For realistic representation of the magnitude of large-scale wind stress and heat flux variability, Miller and Roads found that ocean current advection and anomalous heat flux had comparable importance in driving model SST anomalies. This may be an overemphasis of the effects of currents since Frankignoul and Reynolds (1983), Luksch et al. (1990), and Cayan (1990), among others, have shown that heat fluxes can explain the greatest fraction, although less than approximately half, of the variance of observed SST anomalies. Haney (1980, 1985), on the other hand, has shown that current advection makes an important contribution to the development of model North Pacific SST anomalies, which he found to be correlated with observations.

The structure of the SST anomalies in the present model depends on the structure of the forcing function. Since the heat flux is assumed to be proportional to the air–sea temperature difference, SST anomalies driven by heat flux alone have O(3000 km) length scales commensurate with the length scales of the atmospheric temperature variability. Ekman-induced anomalies (Fig. 1b) have much larger spatial scale than the geostrophic-induced anomalies (Fig. 1a) and presumably couple more efficiently to the thermal field of the atmosphere. In the following discussion, therefore, Ekman-induced anomalies are likely to be more important than geostrophically induced anomalies in influencing large-scale air–sea interaction.

3. Analysis of model output

For both cases, 72 months of coupled model output from the Pacific Ocean sector were analyzed by computing EOFs of a variety of monthly mean model variables, including SST, air temperature (T_a), lower-layer atmospheric streamfunction (analogous to the 750-mb height), heat flux, and SST tendency (subsequent month minus antecedent month). The structure of the first several EOFs of the atmospheric variables differed very little between the two cases. This is consistent with the results of Salmon and Hendershott (1976), who found no significant differences in model atmospheric energy cycles with and without coupling to an interactive mixed layer. The first EOF of atmospheric temperature for case 2 (Fig. 3c) has a more elongated, basin-scale structure than for case 1 (Fig. 2c), but the other atmospheric EOFs of case 2, except for some weak scrambling among themselves, substantially resemble the EOFs of case 1. The EOFs of 750-mb height are virtually identical for these two systems.

One would expect the EOFs of SST to be quite different for the two cases, because the rms SST anomaly increases by a factor of two in much of the basin when ocean current advection is included in this model. However, of the top six EOFS, which together account for over 90% of the variance in each case, only the first EOF of SST (Fig. 3a) appears to be unique to case 2. The other EOFs of case 2 occur with rather similar shapes to those of case 1 (e.g., Figs. 2b, 3b). They are apparently only weakly deformed by the presence of ocean currents.

The cross correlation, however, between the time series of EOFs of the atmospheric variables and SST differs for the two cases. For example, in case 1 the largest-scale EOFs of atmospheric temperature and SST are correlated (in time and in spatial structure) in a one-to-one fashion (Table 1). For case 2 the cross correlations of the EOF time series (Table 2), as well as the spatial structure, reveal less distinct correspondence because the inclusion of ocean current advection scrambles the relations between the EOFs. This is not always true, as evidenced, for example, by the second EOF of air temperature in case 2 (not shown but analogous to Fig. 2d), which seems to force a nearly pure heat flux response in SST (third EOF, analogous to Fig. 2a), virtually identical to the response in case 1 (second EOF of T_a forcing the first EOF of SST).

a. Does standard lagged cross-correlation analysis reveal the fact that anomalous SST forces the atmosphere?

Consider Tables 1 and 2, which list the square of the lagged cross correlation of the EOF coefficient time series of the monthly means of SST and air temperature over the model Pacific. For negative lags, such that atmosphere forces ocean, we see a maximum in the squared correlation. For simultaneous correlations, the squared correlations are reduced but still rather large. For positive lags, such that the ocean leads the atmosphere, we find little or no correlation. These results are entirely consistent with observed cross correlations (e.g., Wallace and Jiang 1987). Shorter time-averaging intervals yielded substantially similar cross-correlation relationships. This suggests that even in a system where midlatitude SST does influence the overlying atmosphere, SST lag correlations with monthly mean atmospheric variables can be expected to fail to indicate significant correlations with positive lags. The intrinsic atmospheric variability of weather obscures the influence of SST. (Similar results hold for the lower-layer streamfunction and SST since the atmospheric response tends to be equivalent barotropic in the sense of hot highs and cold lows.)

b. Does heat flux variability correlate more strongly with SST anomalies or SST anomaly tendency?

Another measure of the influence of ocean upon atmosphere is through analyzing the relationship between heat flux and SST. If heat fluxes are the dominant forcing function in (2.1) so that the ocean responds to atmosphere forcing, then one would expect heat flux to be correlated more strongly with SST tendency. If other processes (such as current advection) drive SST anomalies so that the atmosphere responds to the changing SST, then the heat flux would correlate more strongly with SST. Table 3 (top) lists the squared correlations between the leading EOFs of heat flux and those of the SST tendency from case 2. The results are consistent with those of Cayan (1990), who showed that, throughout the Northern Hemisphere but outside the equatorial strip, observed heat flux anomalies are correlated much better with SST anomaly tendency than SST anomalies themselves (cf. Wallace et al. 1990). A weak correlation between heat flux and SST anomalies, as shown in Table 3 (bottom) for the coupled model, was also found in observations by Frankignoul and Reynolds (1983).

c. Do composites of strong warm/cold events of SST reveal ocean forcing atmosphere?

It is of interest to composite the coupled model output to see if we can obtain results similar to the Ratcliffe

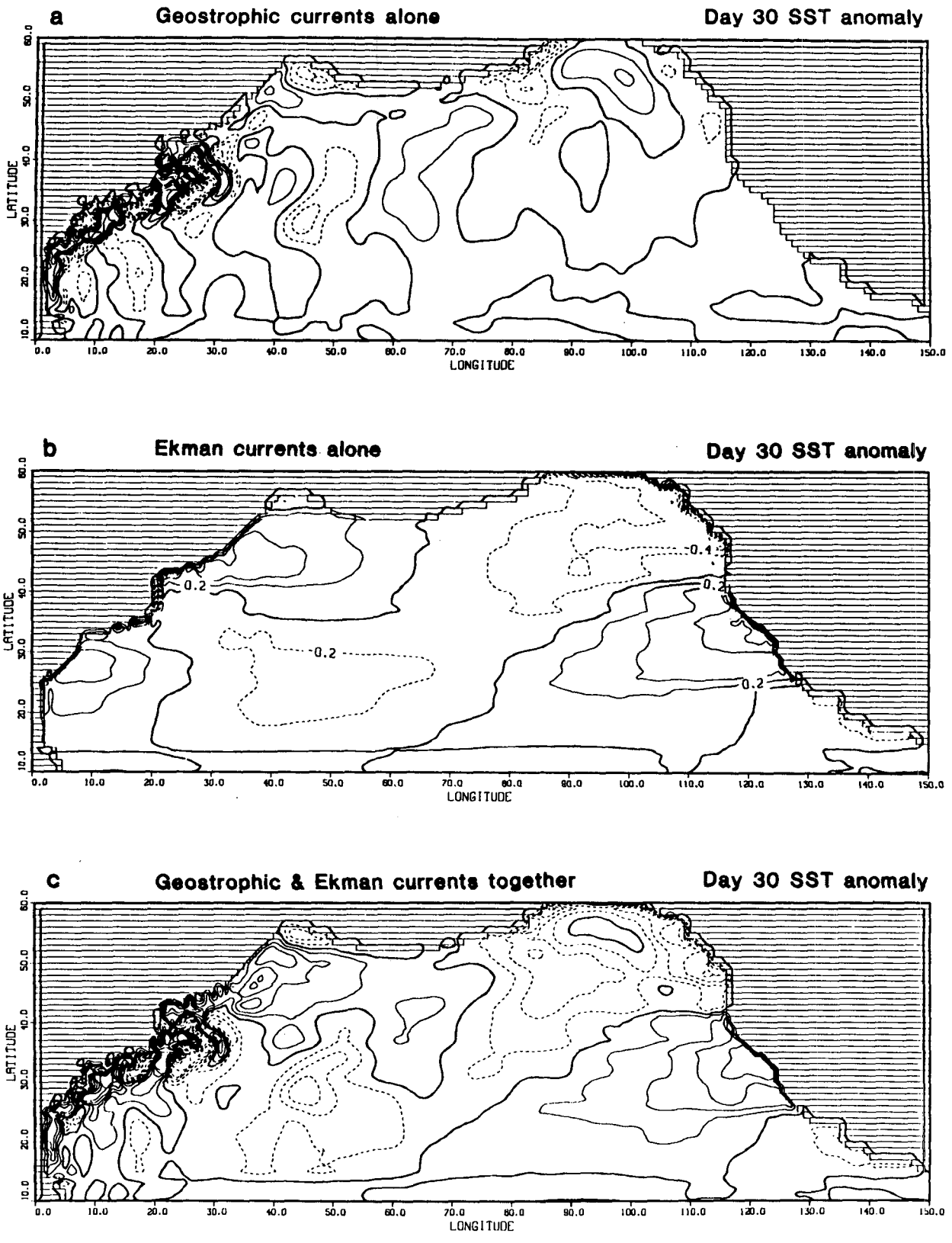

FIG. 1. Examples of the generation of SST anomalies due to time-dependent forcing by ocean currents. In each case the SST anomaly is set initially to zero, based on a 60-month perpetual January climatology. SST anomaly after 30 days of (a) geostrophic current variability alone, (b) Ekman current variability alone, and (c) geostrophic and Ekman current variability combined (contour interval: 0.2°C). The spatial scale discrepancy between Ekman and geostrophic currents is evident in the corresponding SST anomaly fields.

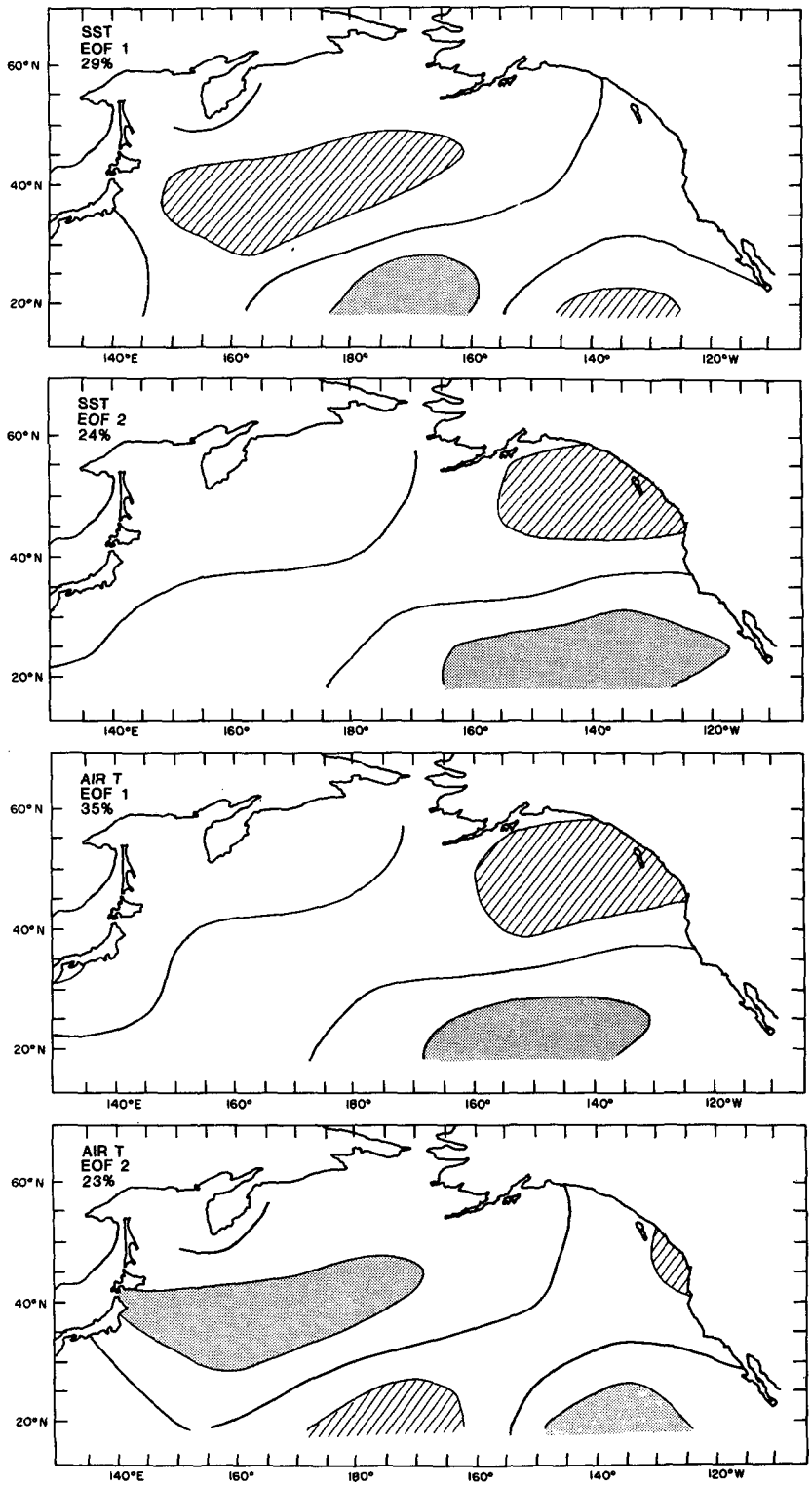

FIG. 2. Empirical orthogonal functions of SST and atmospheric baroclinic streamfunction (air temperature) for case 1, wherein heat fluxes alone contribute to SST variability. (a) SST EOF1, 29% of the variance; (b) SST EOF2, 24%; (c) baroclinic streamfunction EOF1, 35%; and (d) baroclinic streamfunction EOF2, 23% (CI: arbitrary). As evident in Table 1, SST EOF1 and EOF2 are directly related to the baroclinic streamfunction EOF2 and EOF1, respectively.

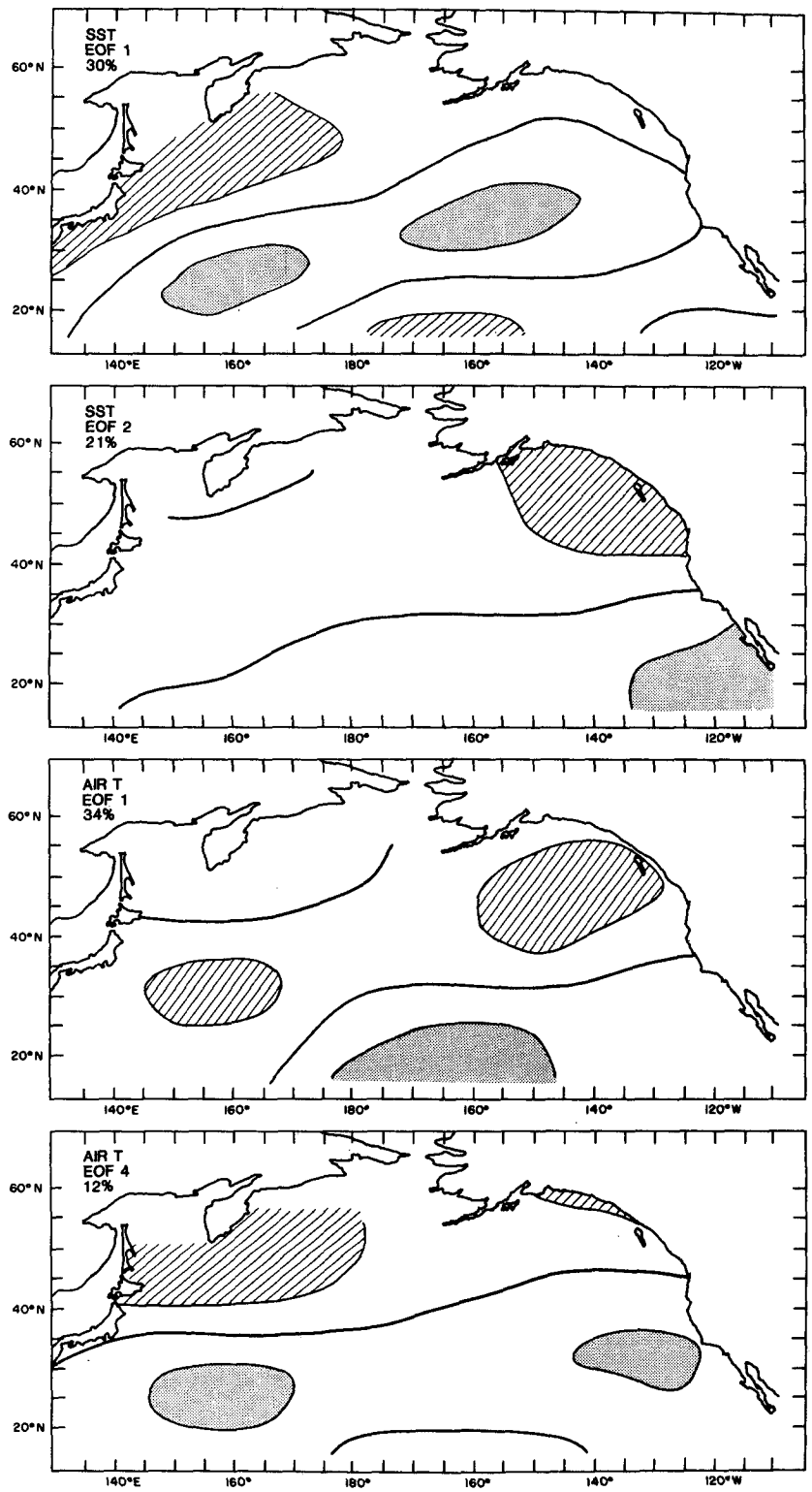

FIG. 3. As in Fig. 2, but for case 2, wherein heat fluxes and ocean current advection contribute to SST variability. (a) SST EOF1, 30% of the variance; (b) SST EOF2, 21%; (c) baroclinic streamfunction EOF1, 34%; and (d) baroclinic streamfunction EOF4, 12% (CI: arbitrary). As seen in Table 2, these four EOFs form an interactive set in the model response. Note that baroclinic streamfunction is correlated, in the sense of hot highs and cold lows, with lower-layer streamfunction from which wind stress and, hence, the Ekman current field is derived.

TABLE 1. Squared correlation between model EOF coefficient time series for baroclinic streamfunction (AIRT) versus sea surface temperature (SST). Case 1: Heat flux only.

	SST EOF1	SST EOF2	SST EOF3	SST EOF4	SST EOF5
		Lag = −1 month			
AIRT EOF1	—	.45	—	—	—
AIRT EOF2	.60	—	—	—	—
AIRT EOF3	—	—	.53	—	—
AIRT EOF4	—	—	—	.46	—
AIRT EOF5	—	—	—	.19	.15
		Lag = 0 months			
AIRT EOF1	—	.15	—	—	—
AIRT EOF2	.34	—	—	—	—
AIRT EOF3	—	—	.42	—	—
AIRT EOF4	—	—	—	.13	—
AIRT EOF5	—	—	—	—	—
		Lag = +1 month			
AIRT EOF1	—	—	—	—	—
AIRT EOF2	—	—	—	—	—
AIRT EOF3	—	—	.16	—	—
AIRT EOF4	—	—	—	—	—
AIRT EOF5	—	—	—	—	—

(— indicates squared correlation less than 0.10)

and Murray (1970) observations (section 1), in which ocean leads atmosphere, exemplifying the ocean forcing atmosphere. Consider the first EOF of SST (Fig. 3a) for case 2, which is of particular interest since it is influenced by both heat flux and current advection. Based on the SST anomaly at the location of the peak amplitude at 38°N 150°W, we extracted all months in which the SST anomaly was greater/less than critical values[2] of ±1.2°C for warm/cold composites. Atmospheric composites of baroclinic streamfunction were then formed for the antecedent, contemporaneous, and subsequent months.

Ten warm months and nine cold months occurred satisfying our SST criterion. Not all of the months of the composites may be considered independent since two pairs of sequential cold months occurred and the 10 warm months occurred as a 4-month sequence and two 3-month sequences. (These persistent episodes of warm SST are discussed later.) However, the one-month lagged autocorrelation for the atmospheric monthly means is roughly 0.2 (as found for the observed atmosphere by Davis 1976) for the 72-month record, averaged over the Pacific sector. If the record is broken up into subsets, identified by months of ex-

TABLE 2. Squared correlation between model EOF coefficient time series for baroclinic streamfunction (AIRT) versus sea surface temperature (SST). Case 2: Heat flux and ocean current advection.

	SST EOF1	SST EOF2	SST EOF3	SST EOF4	SST EOF5
		Lag = −1 month			
AIRT EOF1	.27	.26	—	—	—
AIRT EOF2	—	—	.52	—	—
AIRT EOF3	—	—	—	.13	.16
AIRT EOF4	.23	.23	—	—	—
AIRT EOF5	—	—	—	.15	.14
		Lag = 0 months			
AIRT EOF1	.16	.11	—	—	—
AIRT EOF2	—	—	.27	—	—
AIRT EOF3	—	—	—	—	—
AIRT EOF4	.15	.12	—	—	—
AIRT EOF5	—	—	—	.12	.12
		Lag = +1 month			
AIRT EOF1	—	—	—	—	—
AIRT EOF2	—	—	—	—	—
AIRT EOF3	—	—	—	—	—
AIRT EOF4	—	—	—	—	—
AIRT EOF5	—	—	—	—	—

(— indicates squared correlation less than 0.10)

[2] The results do not depend strongly on the chosen critical value of ±1.2°C in SST because of the trade-off between statistical reliability, which increases with sample size, and the strength of atmospheric response, which decreases with SST anomaly size.

TABLE 3. Squared correlation between model EOF coefficient time series for heat flux (Q) versus SST tendency (ΔSST) and SST. Case 2: Heat flux and ocean current advection.

	ΔSST EOF1	ΔSST EOF2	ΔSST EOF3	ΔSST EOF4	ΔSST EOF5
			Lag = 0 month		
Q EOF1	.38	—	—	—	—
Q EOF2	—	—	.17	.20	—
Q EOF3	—	.13	.16	.15	—
Q EOF4	—	.35	.10	—	—
Q EOF5	—	—	—	—	.46
			Lag = 0 month		
Q EOF1	—	—	—	—	—
Q EOF2	—	—	—	—	—
Q EOF3	—	—	—	—	—
Q EOF4	.17	—	—	—	—
Q EOF5	—	—	—	—	—

(— indicates squared correlation less than 0.10)

treme SST, moderate SST, weak SST, and near-normal SST, the lagged autocorrelation of the atmosphere for each subset is not significantly different from the value from the entire record. Therefore, we assume that the N months contributing to the atmospheric composites are composed of N independent samples.

To obtain a measure of significance, a t test was performed to determine whether a composite ensemble mean, μ, differs significantly from the 72-month ensemble mean of the entire record. Since the basic mean is zero,

$$t = \frac{\mu}{\sigma^* \sqrt{N_1^{-1} + N_2^{-2}}},$$

where

$$\sigma^* = \left(\frac{N_1 \sigma_1^2 + N_2 \sigma_2^2}{N_1 + N_2 - 2} \right)^{1/2}$$

is the weighted standard deviation with $N_1 = 10$ (warm composite) and $N_2 = 72$. Thus, $\sigma^* \approx \sigma_2$ and $t \approx \mu / \sigma_2 \sqrt{1/N_1 + 1/N_2}$. Assuming that there are 70 degrees of freedom in a two-sided test, an estimate, μ, having a t value greater than 2.0 is 95% likely to be nonzero. In Figs. 4 and 5, a grid point at which the atmospheric field estimate is significant at or greater than the 95% level is indicated by an asterisk.

For both the warm and cold composites, the antecedent month's atmospheric pattern (Figs. 4b, 5b) has the largest response and has a pattern very similar to the SST composite (Figs. 4a, 5a), indicative of atmosphere forcing ocean. The contemporaneous atmospheric composites for the warm (Figs. 4c, 5c) and cold SST events are smaller in amplitude but are still very similar in structure to the SST. The warm composite contemporaneous atmospheric response is significant at the 95% level, while the cold contemporaneous response is only significant at the 90% level.

For the subsequent month of the warm composite there is a significant atmospheric response (Fig. 4d) that is shifted eastward, and slightly northward, of the maximum SST. This result is consistent with the observations of Ratcliffe and Murray (1970) and the modeling results of Palmer and Sun (1985), who forced the ECMWF model with fixed SST anomalies (designed after the Ratcliffe–Murray Atlantic observations) and showed a significant shift in the atmospheric response compared to flow over the climatic SST. These results support the idea that compositing extreme events of SST can demonstrate the ocean forcing atmosphere.

In contrast to the significant response in the subsequent month for the warm composite, the subsequent month for the cold composite (Fig. 5d) yields only a weak cold atmospheric anomaly over the southwest United States, which is not significant. Although nonsymmetric atmospheric responses to warm/cold anomalies are possible (e.g., Pitcher et al. 1988 found a low pressure atmospheric model response over both cold and warm fixed SST anomalies; Roads 1989 found asymmetric responses to fixed SST anomalies in some regions of the globe), as a result of, for example, the self advection of the anomalous atmospheric flow, it is puzzling why the subsequent month of the cold case differs from that of the warm case. It may simply be because the SST cold events of the model are more prevalent and are consequently of smaller magnitude than the warm events. Namias et al. (1988) show that strong SST anomalies tend to be associated with persistence of both atmosphere and ocean, which corroborates the model results, showing that the (weaker) cold SST events appear to be associated with less persistent atmospheric anomalies than the (stronger) warm SST events. However, there is no observational evidence that cold SST events are less persistent or weaker than warm SST events (indeed the reverse may be true; Namias 1979; Namias et al. 1988). Either statistical chance or, more likely, the simplicity of the model may be the cause of the discrepancy between the subsequent months of warm and cold cases.

Composites of the lower-layer streamfunction (not illustrated) may help to further distinguish the warm and cold cases. For the antecedent, contemporaneous, and subsequent months of the warm composite, the atmospheric response corresponds to hot highs, with the thermal response being strongly in phase with the lower-level high pressure. The cold low of the antecedent month of the cold composite also is spatially in phase. But for the contemporaneous month of the cold

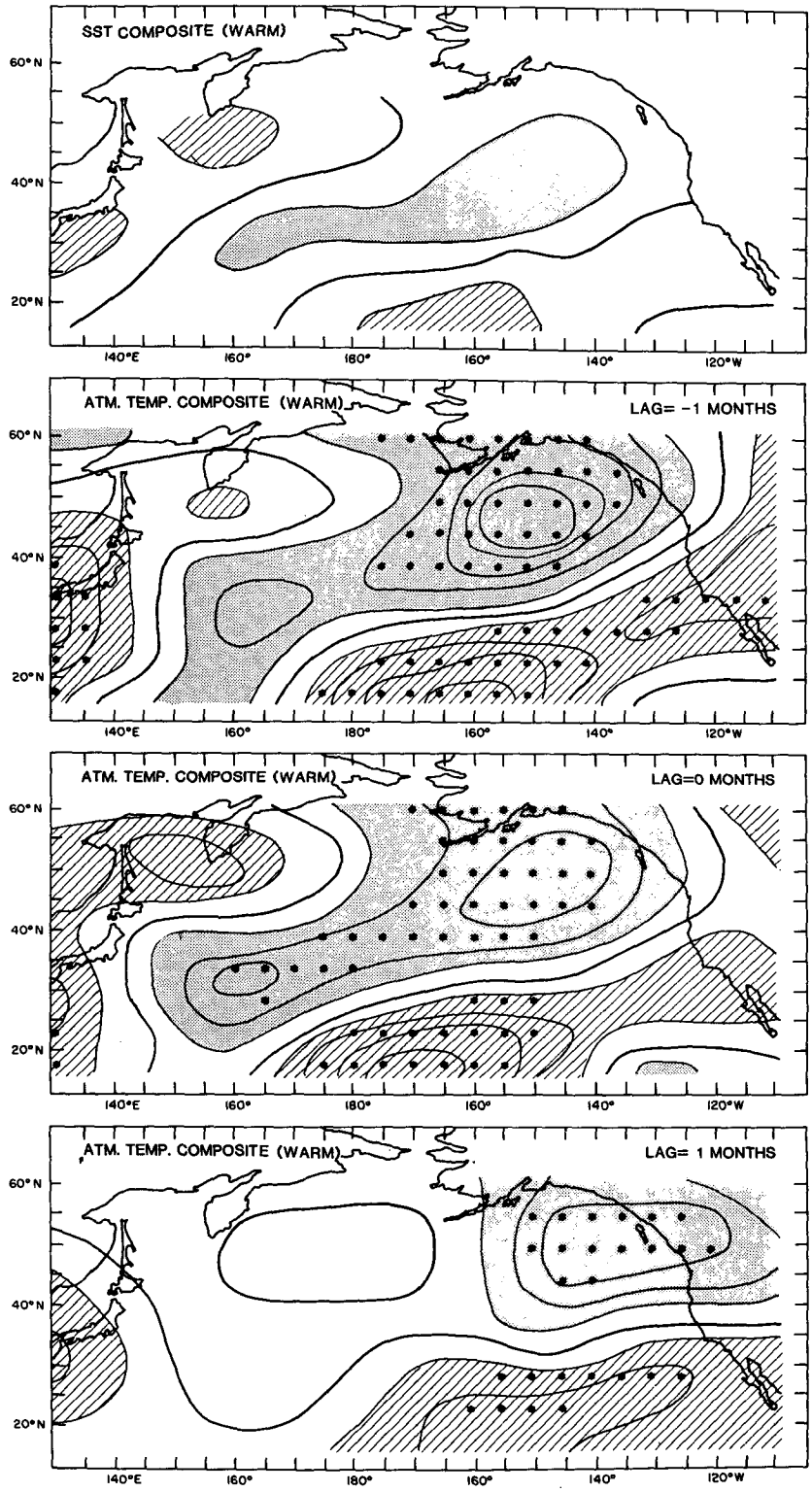

FIG. 4. Case 2 results for compositing monthly means associated with warm SST anomalies ($\geq$1.2°C at the point 38°N, 150°W, resulting in 10-member ensemble). (a) SST composite (CI = 1°C, peak value = 1.8°C), (b) baroclinic streamfunction for antecedent month (CI: 5.9×10^5 m^2 s^{-1}), (c) Baroclinic streamfunction for contemporaneous month (CI: 5.9×10^5 m^2 s^{-1}), (d) baroclinic streamfunction for subsequent month (CI = 5.9×10^5 m^2 s^{-1}). Shading (hatching) indicates positive (negative) values. Grid points indicated by an asterisk indicate significance at or above the 5% level.

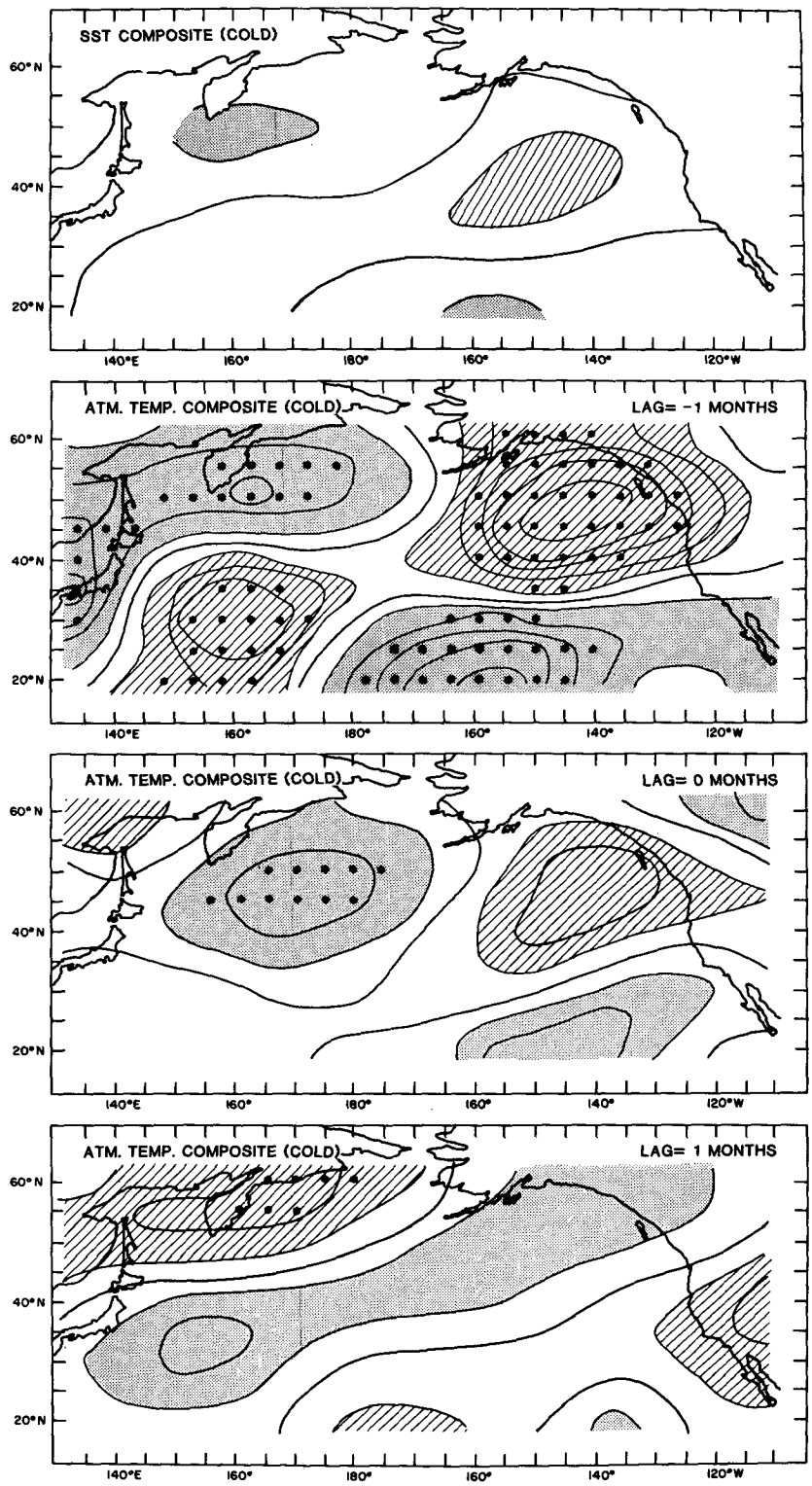

FIG. 5. As in Fig. 4, but composites are associated with cold SST anomalies (≤ -1.2°C at the point 38°N, 150°W, resulting in a 9-member ensemble). (a) SST composite (CI = 1°C, peak value = 1.5°C), (b) baroclinic streamfunction for antecedent month (CI = 5.9×10^5 m^2 s^{-1}), (c) baroclinic streamfunction for contemporaneous month (CI = 5.9×10^5 m^2 s^{-}), (d) baroclinic streamfunction for subsequent month (CI = 5.9×10^5 m^2 s^{-1}). In (c), the cold atmospheric anomaly overlying the cold SST anomaly is significantly nonzero only at the 10% level.

events, the lower-level high is shifted southward with respect to the air temperature field. This southward positioning of the high pressure affects the pattern of Ekman velocity and may affect the resultant SST anomaly evolution, especially insofar as the Palmer–Sun mechanism occurs, as discussed in the next subsection.

d. Does the presence of ocean current advection in ocean–atmosphere interaction result in regions of enhanced persistence in the manner described by Palmer and Sun (1985)?

Case 2 includes the basic features of the Palmer–Sun enhanced persistence effect; namely, air–sea heat exchange and Ekman advection of SST anomalies, though it fails to include the effect of wind speed on heat exchange. The inclusion of ocean current forcing of SST might be expected to deteriorate the persistence of model SST anomalies generated by heat fluxes, for example, because of the smaller spatial scales of SST generated by fluctuating geostrophic currents. Indeed, in the western region of the basin, where geostrophic currents generate substantial SST anomalies, total SST and EOFs of SST associated with this region are less persistent in case 2 than total SST or the EOF analogs of case 1. It follows that atmospheric persistence due to the Palmer–Sun mechanism does not arise in the western region of the model basin.

In the eastern basin, however, the dominant EOF of SST for case 2 has its center of action and potentially could exhibit enhanced persistence because it is clearly influenced by Ekman current advection. We therefore direct attention to the northeastern Pacific (33°–43°N, 145°–170°W), defined by the maximum of the first EOF of SST (Fig. 3a), which accounts for 30% of the variance. The squared lagged autocorrelations for SST in the two cases are shown in Table 4 for one-month, two-month, and three-month lags. It is evident that persistence of monthly averaged SST anomalies is enhanced in the open ocean in the northeastern basin in the case where ocean currents affect SST anomalies.

This result must be interpreted cautiously, particularly because there is no analog EOF of SST in this region in case 1. It may simply be that since there is no organized response in this region in case 1, the SST deteriorates more quickly due to disorganized forcing. Table 5 shows the squared lagged autocorrelations for the SST EOFs of both cases. The first EOF of case 2 is more persistent than the first EOF of case 1. This supports the idea that an enhancement to persistence of SST is occurring in the northeast Pacific. Additionally, the second EOF of SST for case 2, which has its center of action in the eastern Pacific and is linked to EOF1 through mutual atmospheric forcing, is more persistent than its analog, EOF2, in case 1. This further supports the enhanced SST mechanism. Note, however, that EOF3 of SST from case 2, which is the analog of EOF1 from case 1, is less persistent than in case 1. This is apparently because its center of action is in the western basin where geostrophic current forcing may help to decorrelate the SST pattern.

TABLE 4. Squared autocorrelation of SST anomalies for the region 33°–43°N, 145°–170°W.

	Lag		
	1 month	2 months	3 months
Case 1: Heat flux only	.38	.05	.00
Case 2: Heat flux and current advection	.53	.21	.05

TABLE 5. Squared autocorrelation of SST anomaly EOF time series.

	Lag		
	1 month	2 months	3 months
	Case 1		
EOF1	.67	.36	.15
EOF2	.64	.30	.12
EOF3	.58	.13	.00
	Case 2		
EOF1	.65	.28	.06
EOF2	.46	.13	.01

Therefore, the result of Table 4 is only suggestive evidence supporting the mechanism of Palmer and Sun. Indeed, we found virtually no evidence for enhancement of persistence of the *atmosphere* over the northeast Pacific in lagged autocorrelation for 5-day, 10-day, . . . , through 90-day averages in case 2 versus case 1. The only scrap of an enhancement was that EOF 4 of air temperature for case 2 exhibited a significant squared autocorrelation of 0.13, for a lag of 1 month, compared to nil in case 1. Thus, although section 4c showed that composites of atmospheric response can show a significant relationship to warm SST events of the previous month, synoptic-scale noise can obscure that signal when examining the entire 72-month record.

Since Palmer and Sun (1985) discussed only briefly the manner in which warm water is advected northward by the anomalous atmospheric flow, we further address their argument of SST anomaly reinforcement by Ekman currents. In this model, heat fluxes caused by a circularly symmetric air temperature anomaly attempt to generate an SST anomaly that is spatially in phase (Fig. 6a) with the air temperature field, as found for example in case 1. If Ekman currents are important, then Ekman advection will force (on an f plane) an antisymmetric perturbation to SST as shown in Fig. 6b, because the model baroclinic streamfunction tends to be correlated with lower-layer streamfunction in the

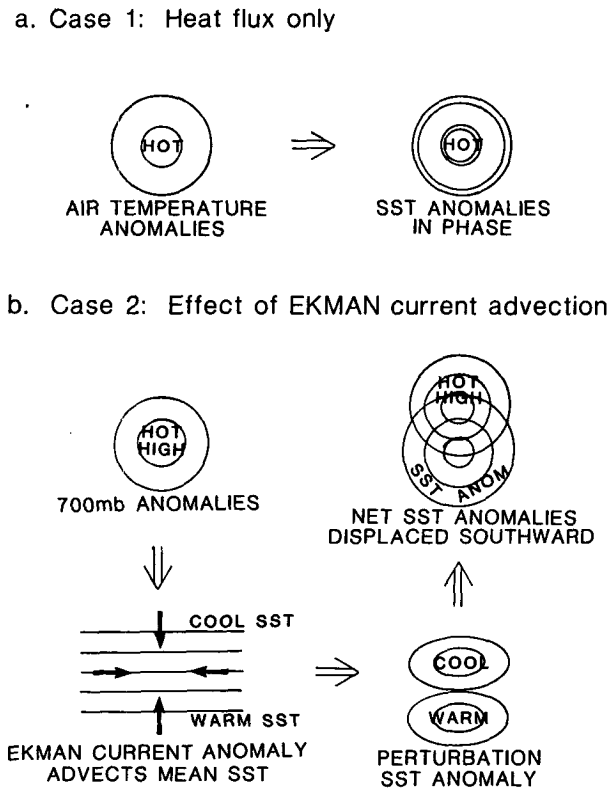

FIG. 6. Schematic of the SST anomaly response to a fixed, circularly symmetric perturbation of model atmospheric baroclinic streamfunction on an f plane. (a) When heat fluxes alone affect SST, the SST anomaly is in phase with the baroclinic streamfunction anomaly. (b) When Ekman currents are included, the lower-layer streamfunction (in phase with the baroclinic streamfunction in the sense of hot highs and cold lows) drives anomalous currents against the background mean SST gradient, which results in an antisymmetric SST anomaly perturbation to the heat flux SST anomaly response. Consideration of the case of latitudinally dependent f (see text) suggests that the southern part of this perturbation is stronger than the northern part.

sense of hot highs and cold lows. Thus, the net SST anomaly does not strictly reinforce the warm air temperature anomaly, as suggested by Palmer and Sun, because the net SST anomaly is displaced southward of the atmospheric anomaly. Indeed, in case 2, the first EOF of SST appears to exhibit structures that are displaced southward (and westward) of the overlying atmospheric forcing (Fig. 3a,c).

But if the Coriolis frequency is a function of latitude, then the strength of the Ekman advection velocity ($\mathbf{k} \times \tau/\rho_0 f H$) is stronger to the south of a circularly symmetric atmospheric anomaly. Second, the wind stress associated with a symmetric perturbation in geopotential height is also asymmetric, in the sense that wind anomalies (proportional to f^{-1} by the geostrophic relation), and hence those of wind stress, are also stronger to the south side of a circular height anomaly. Both of these effects are included in the coupled model. Thus, the net Ekman-forced SST anomaly perturbation is not quite like Fig. 6b but is asymmetric, being more strongly reinforced to the south and less strongly diminished to the north. This argument lends more support to the Palmer and Sun mechanism but still results in a net southward displacement of either warm or cold SST anomalies.

Continuing this argument, the response of the atmosphere to the "new" SST anomaly tends to be either downstream (as in Palmer and Sun's atmospheric model) or to the northeast of the SST anomaly (as in the observations of Ratcliffe and Murray 1970, the coupled model results of Salmon and Hendershott 1976, and in the present coupled model). Thus, the net result of the time-varying ocean–atmosphere interaction may produce an easterly migration of the anomalous system. Indeed, Frankignoul (1985) analytically solved a simplified coupled model, similar to the model of case 1, and found eastward propagation of anomalies. The main difference with case 1 is that Frankignoul considered a linear atmospheric model, which as shown by Roads (1989) for the present model, yields different atmospheric 700-mb pressure responses to fixed SST anomalies from its synoptically active nonlinear analog. The *thermal* response, however, tends to be similar so that eastward migration may occur in a similar way in both models. Eastward migration of observed SST anomalies has been discussed by Namias (1972b), who pointed out that SST anomalies migrate northeastward over seasonal time scales. The enhanced persistence mechanism is also supported by the results of Pedlosky (1975), who examined an analytical coupled model (the dynamics of which is contained within our simplified system), which showed that seed SST anomalies can grow due to an unstable air–sea interaction.

Returning to the puzzle of why the cold composites fail to yield a significant response, it is possible that the phasing of the air temperature and lower-level pressure for the contemporaneous atmospheric cold composite is of central importance. On average, as evidenced in the composites of cold events, the atmosphere appears to respond with the surface low pressure displaced to the south of the cool air temperature anomaly, causing the Ekman advection effect to dampen the local cold SST anomaly and force a cold SST anomaly response that is too far south of the local atmospheric anomaly to have a substantial effect. Thus, the positive feedback mechanism may be suppressed during cold events because of an asymmetry in the contemporaneous atmospheric response to warm versus cold events of SST.

4. Summary

In a previous paper, which analyzed the coupled model discussed here, Miller and Roads (1990) showed that forcing the atmospheric model with SST anomalies taken from a base run of the coupled system resulted

in significant improvements in hindcasting the original coupled model atmospheric anomalies. (The atmospheric model was able to hindcast approximately 25% of the variance of monthly through 3-monthly averages of Pacific baroclinic streamfunction when forced by the "observed" SST anomalies.) Despite that demonstration of oceanic SST forcing, the dominant signal from the statistical analyses employed in this paper is that of atmosphere driving ocean (Tables 1–3; Figs. 4, 5).

The results of the present study vividly show how difficult it is to prove that real SST anomalies strongly influence the midlatitude atmospheric flow field when using standard statistical techniques. Since theoretical predictability studies cannot be done with the real atmosphere, we must rely on sophisticated atmospheric forecast models used in a hindcasting mode, with and without observed SST anomaly forcing, that can then be verified or vilified with observations. But such studies are indefinitive because of deficiencies in the atmospheric models and the limited number of experiments that can be executed.

Composites of strong model SST anomaly events, however, were identified in this study as useful indicators of ocean forcing atmosphere. In agreement with the observations of Ratcliffe and Murray (1970), there was a relatively large, phase-shifted atmospheric response in the month subsequent to the strong warm SST composite (Fig. 4d). The cold SST events failed to correspond to a significant atmospheric response in the subsequent month, possibly because of their lower amplitude or because of the asymmetry in atmospheric response to warm/cold forcing; cold (warm) SST forced contemporaneous lower-layer streamfunction anomalies that appeared to be out of (in) phase with baroclinic streamfunction anomalies.

We also compared output from two cases of our coupled model (with and without ocean current advection), to attempt to determine the effect of ocean current advection on large-scale, midlatitude, air–sea interaction. We identified an enhancement to SST persistence (but not atmospheric persistence) in the case where ocean currents influence SST (Tables 4, 5), supportive of the scenario of Palmer and Sun (1985). There were very few other differences between those two coupled systems, one difference being the unique first mode of SST variability (Fig. 3a) and another being the scrambling of the relationships between atmospheric variables and SST (Table 2).

Since correlations are such a poor indicator of the ocean driving the atmosphere, we suggest the influence of the ocean upon the atmosphere can be better determined by isolating the large-scale air–sea interactions that may occur in coupled models vis à vis nature. To achieve further progress, more sophisticated models, which include more complete physical processes, must be developed. The coupled midlatitude model system considered herein neglects several physical processes that may alter the results: (i) There is no hydrological cycle in the system and the heat flux parameterization thereby ignores latent heat exchange. (ii) Heat flux depends on the wind speed, unlike the linear heat exchange relation invoked in this model. (iii) The effects of turbulent entrainment and convective overturning have been excluded from the ocean component of the coupled model. These oceanic processes are particularly important insofar as we have left out (iv) the transition of the seasons, which is potentially a vital effect (Namias 1976; Davis 1978 vis à vis 1976).

Acknowledgments. Support was provided by NOAA Grants NA86-AA-D-CP104 and NA90AA-D-CP526, NASA Grant NAG5-236, the University of California INCOR Program for Global Climate Change, and the Vettleson Foundation. Supercomputing resources at the San Diego Supercomputer Center were provided by a grant from SDSC and the SIO Block Grant. Dan Cayan and John Roads generously provided inspiration, computer codes, and discussions that sparked many aspects of this investigation. Marguerette Shultz drafted the figures. I thank Dan Cayan, John Roads, Phil Bogden, Mark Swenson, and the two perceptive referees for comments on the manuscript.

REFERENCES

Cayan, D. R., 1990: Variability of Latent and Sensible Heat Fluxes over the Oceans. Ph.D. dissertation, University of California, San Diego, 199 pp.

Chervin, R. M., J. E. Kutzbach, D. D. Houghton, and R. G. Gallimore, 1980: Response of the NCAR general circulation model to prescribed changes in ocean surface temperature. Part II. Midlatitude and subtropical changes. *J. Atmos. Sci.*, **37**, 308–332.

Davis, R. E., 1976: Predictability of sea surface temperature and sea level pressure anomalies over the North Pacific Ocean. *J. Phys. Oceanogr.*, **6**, 249–266.

——, 1978: Predictability of sea level pressure anomalies over the North Pacific Ocean. *J. Phys. Oceanogr.*, **8**, 233–246.

Frankignoul, C., 1985: Sea surface temperature anomalies, planetary waves, and air–sea feedback in the middle latitudes. *Rev. Geophys.*, **23**, 357–390.

——, and R. W. Reynolds, 1983: Testing a dynamical model for midlatitude sea surface temperature anomalies. *J. Phys. Oceanogr.*, **13**, 1131–1145.

Haney, R. L., 1980: A numerical case study of the development of large-scale thermal anomalies in the central North Pacific Ocean. *J. Phys. Oceanogr.*, **10**, 541–556.

——, 1985: Midlatitude sea surface temperature anomalies: A numerical hindcast. *J. Phys. Oceanogr.*, **15**, 787–799.

Lau, N-C., and M. J. Nath, 1990: A general circulation model study of the atmospheric response to extratropical SST anomalies observed in 1950–79. *J. Climate*, **3**, 965–989.

Luksch, U., H. von Storch, and E. Maier-Reimer, 1989: Modeling North Pacific SST anomalies as a response to anomalous atmospheric forcing. Max-Planck-Institut für Meteorologie, Hamburg, Report No. 37, 31 pp.

Miller, A. J., and J. O. Roads, 1989: A simplified coupled model of extended-range predictability. *J. Climate*, **3**, 523–542.

Namias, J., 1963: Large-scale air–sea interactions over the North Pacific from summer 1962 through the subsequent winter. *J. Geophys. Res.*, **68**, 6171–6186.

——, 1972a: Large-scale and long-term fluctuations in some atmospheric and oceanic variables. *Nobel Symposium 20,* D. Dyrssen and D. Jagner, Eds. Almquist and Wiksell, Stockholm, 27–44.

——, 1972b: Experiments in objectively predicting some atmospheric and oceanic variables for the winter of 1971–72. *J. Applied Meteor.,* **11,** 1164–1174.

——, 1976: Negative ocean–air feedback systems over the North Pacific in the transition from warm to cold season. *Mon. Wea. Rev.,* **104,** 1107–1121.

——, 1978: Recent drought in California and Western Europe. *Rev. Geophys. Space Phys.,* **16,** 435–458.

——, 1979: Northern Hemisphere seasonal 700 mb height and anomaly charts, 1947–1978, and associated North Pacific sea surface temperature anomalies. CALCOFI Atlas No. 27, Scripps Institution of Oceanography, 275 pp.

——, X. Yuan, and D. R. Cayan, 1988: Persistence of North Pacific sea surface temperature and atmospheric flow patterns. *J. Climate,* **1,** 682–703.

Palmer, T. N., and Z. Sun, 1985: A modelling and observational study of the relationship between sea surface temperature in the north-west Atlantic and the atmospheric general circulation. *Quart. J. Roy. Meteor. Soc.,* **111,** 947–975.

Pedlosky, J., 1975: The development of thermal anomalies in a coupled ocean–atmosphere model. *J. Atmos. Sci.,* **32,** 1501–1514.

Pitcher, E. J., M. L. Blackmon, G. Bates, and S. Muñoz, 1988: The effect of North Pacific sea-surface temperature anomalies on the January climate of a general circulation model. *J. Atmos. Sci.,* **45,** 173–188.

Ratcliffe, R. A. S., and R. Murray, 1970: New lag associations between North Atlantic sea temperature and European pressure applied to long-range forecasting. *Quart. J. Roy. Meteor. Soc.,* **96,** 226–246.

Roads, J. O., 1989: Linear and nonlinear responses to middle latitude surface temperature anomalies. *J. Climate,* **2,** 1014–1046.

Salmon, R., and M. C. Hendershott, 1976: Large-scale air–sea interactions with a simple general circulation model. *Tellus,* **28,** 228–242.

Wallace, J. M., and Q. Jiang, 1987: On the observed structure of the interannual variability of the atmosphere/ocean climate system. *Atmospheric and Oceanic Variability,* Roy. Meteor. Soc., H. Cattle, Ed., 17–43.

——, C. Smith, and Q. Jiang, 1990: Spatial patterns of atmosphere–ocean interaction in the northern winter. *J. Climate,* **3,** 990–998.